論文 / 著書情報
Article / Book Information

Title	Study on Self-contained and Terrain Adaptive Active Cord Mechanism
Author	Gen Endo, Keiji Togawa, Shigeo Hirose
Journal/Book name	Proc. of International Conference on Intelligent Robots and Systems '99, Vol. , No. , pp. 1399-1405
発行日 / Issue date	1999,
権利情報 / Copyright	(c)1999 IEEE. Personal use of this material is permitted. However, permission to reprint/republish this material for advertising or promotional purposes or for creating new collective works for resale or redistribution to servers or lists, or to reuse any copyrighted component of this work in other works must be obtained from the IEEE.

Proceedings of the 1999 IEEE/RSJ
International Conference on
Intelligent Robots and Systems

Study on Self-contained and Terrain Adaptive Active Cord Mechanism

Gen ENDO, Keiji TOGAWA *and* Shigeo HIROSE

Dept.of Mechano-Aerospace Eng., Tokyo Institute of Technology
2-12-1 O-okayama Meguro-ku Tokyo 152-8552 Japan
E-mail: endo@mes.titech.ac.jp, togawa@mes.titech.ac.jp, hirose@mes.titech.ac.jp

Abstract

A snake is able to attain high terrain adaptability and versatile locomotion even though it has an extremely simple one-dimensional configuration. In order to utilize these functions for robotics, we have adapted the basic biological machine elements of the snake into the Active Cord Mechanism (ACM). And we have discussed the creeping dynamics and applications to manipulation. In this paper, we developed a new experimental model named "ACM-R1" with a self-contained system, which realizes higher mobility and terrain adaptability compared with the past model. Next, gliding experiments on ice were carried out in order to demonstrate that the creeping motion is the same as the principle of skating. Finally, a new terrain adaptive control method for sloping surfaces is proposed, and we verified the effectiveness of it by slope climbing experiments.

1. Introduction

A snake is able to attain high terrain adaptability and versatile locomotion even though it has an extremely simple one-dimensional configuration. It is extremely useful to apply such functions to robotics. We have adapted the basic biological machine elements of the snake into the Active Cord Mechanism (ACM). We have discussed the creeping dynamics and applications to manipulation [1]. In particular, we analyzed the creeping motion and the results were compared with animal experiments. In addition, a mechanical model named "ACM III" was introduced and the creeping motion was demonstrated on level ground.

However, the verification of the creeping motion by the mechanical model in the past remains qualitative and quantitative considerations have not been performed. Moreover, the research motive itself occurred from the viewpoint of scientific and biomechanic clarification of the snake locomotion.

In this study, our final goal is the construction of the motion control algorithm, which can be applied to real mechanical models with limitations such as actuator power and mechanical restraints. We will investigate the motion control methods for the mechanical model of ACM from here forth.

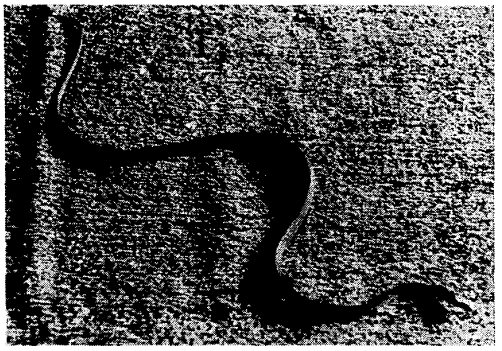

Photo.1 Creep movements of a snake

In this paper, we developed a new self-contained experimental model named "ACM-R1", which realizes higher mobility and terrain adaptability compared with ACM III. In addition, gliding experiments on ice were carried out in order to demonstrate that the creeping motion is the same as the principle of skating. Finally, a new terrain adaptive control method for sloping surfaces is proposed, and we verified the effectiveness of it by slope climbing experiments.

2. Kinematics of creeping motion

A snake's body is covered with smooth scales allowing easy sliding. However, when the snake makes creeping motion, the abdomen flank of the body becomes an edge like that of a ski in order to prevent the slippage in the normal direction of the body. So the snake has friction characteristics such that slip is easy along the body but difficult in the normal direction. These characteristics transform the contraction/relaxation motion of the muscle into propulsive creeping motion like the flowing of a river.

The direction along the body axis is determined as the tangential direction and the orthogonal direction of body axis is determined as the normal direction. The nomenclature is shown in Fig.1. For simplicity of the analysis, the conventional gliding theory assumed that: (1) The body is expressed by a continuum. (2) Distribution of torque is independent of the gliding configuration. (3) Analysis by

0-7803-5184-3/99/$10.00 © 1999 IEEE

static kinematics. (4) No slippage in the normal direction. However, these assumptions are not strictly valid, so recently Ma has proposed another analysis, which includes dynamics and normal direction slippage [2] and considers the relationship between the gliding configuration and torque distribution in terms of the muscular power consumption [3].

The serpenoid curve is assumed as the function which represent the gliding configuration. The serpenoid curve is a curve whose curvature changes sinusoidally along the axis of the curve, and it approximates the gliding configuration. s is a distance along axis of the body and $\theta(s)$ is the distribution of the bending angle along body axis. The bending angle at position s with amplitude A is given by

$$\theta(s) = A\sin\left(\frac{\pi}{2}\cdot\frac{s}{l}\right) \tag{1}$$

The definition of winding angle α is the integration of the bending angle from O to P. α is expressed as follows by using incremental length δs.

$$\alpha = \frac{l}{\delta s}\cdot\frac{2}{\pi}\cdot A \tag{2}$$

V_s, velocity in the line of the body axis, is geometrically required by assuming that side-slip does not occur.

$$V_s = \frac{4l}{T} \tag{3}$$

Here, l is the length of the quarter-cycle of the curve and T is a period of the winding. V_x, velocity in the direction of travel is expressed as

$$V_x = V_s\cdot\frac{X(l)}{l} \tag{4}$$

X(l) is the projected length of segment OP in the X-axis of the trunk. So travelling ratio X(l)/l is the ratio at which the speed of motion in the vertebral axis is transferred to the overall locomotion speed of the snake.

The ratio of normal force and tangential force that characterizes the efficiency of the creeping motion is obtained from

$$\frac{F_t}{F_n} = Serp(\sigma)\cdot\alpha \tag{5}$$

Here, $Serp(\sigma)$ is constant ($0.405<Serp(\sigma)<0.637$). This equation indicates that an increase of α results in a larger force distribution in the tangential direction. The torque distribution is determined from the consideration of muscle expansion motion along the trunk. And the distribution of the normal force is obtained only by the second derivative of torque distribution and is independent of the gliding configuration. The shape of the normal force distribution along s is illustrated in Fig.1, where the maximum value is at point O.

μ_t, μ_n are the friction coefficients for the snake's abdomen in the tangential and normal directions respectively. Thus the slip-free creeping motion requires the following conditions.

$$\alpha \geq \frac{1}{Serp(\sigma)}\cdot\frac{\mu_t}{\mu_n} \cong \alpha_0 \tag{6}$$

This equation shows that the friction coefficient ratio determines the minimum α without side slippage. Notice that this equation is necessary but not sufficient.

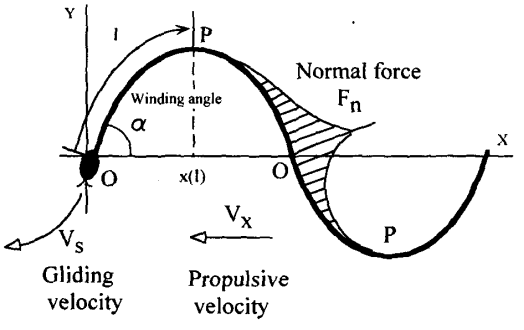

Fig.1 Nomenclature of gliding configuration in regular creeping motion

3. Development of ACM-R1

In this chapter, a new experimental model "ACM-R1" is developed with a non-tethered control system.

3.1 Mechanism

For an artificial creeping machine, the most appropriate structure is probably that of a series of active joints, linked in series. These would correspond to the musculoskeletal system of the snake and the antagonistic muscles connecting them. We made 16 segments with consideration for the size of the mechanisms, discrete error stemming from the discrete structure and the control computer.

In order to perform the creeping motion on a 2 dimensional flat plane, the needed degrees of freedom are only around the normal direction of the gliding surface. Fig.2 shows the installation of the passive wheels to each joint in order to provide the friction characteristics instead of scales. The passive wheel axis is mechanically adjusted such that it always bisects the angle between the nearest segment equally, so as to avoid interference. This mechanism also decreases the discrete error. Because the tangential direction of the wheels are made to follow a path closely approximating a continuous gliding curve by this mechanism. Each joint's work space is ± 35[deg].

Each segment is composed of mechanically equivalent units. These segments are connected serially by a suspension mechanism in order to adapt themselves to the roughness of the gliding surface (Fig.3).

3.2 Sensors

In order to observe the gliding condition, normal direction force, velocity in the line of the body axis and joint torque are measured. The sensor system is shown in Photo.2.

The normal force sensor is composed of a sliding plate which moves along the linear guide in the normal direction, with a coil spring and potentiometer. The passive wheel axis is fixed on the sliding plate which is supported by a coil spring. The normal force is calculated by measuring the displacement using the potentiometer. The velocity v_s is measured by a tacho generator with a small wheel. And the actuator current is measured in order to estimate joint torque. Joint angle is measured by a potentiometer.

These sensors are equipped at the 5th and 13th segments, which are not influenced in the trunk end because the analysis takes no account of the trunk end.

3.3 System configuration

Fig.4 shows the scheme of the control system. The parameters of gliding velocity, direction and amplitude of the bending motion, are transmitted by radio waves. The control computer using these parameters calculates the joint angles. Each joint position is controlled by a servo driver (Titech Robot Driver [4]), so the computer only sends the value of each joint angle. This open loop control method remarkably reduces calculation load of the control computer.

Calculation and output of the commands are carried out by the two small one-board microcomputers (Parallax inc. Basic Stamp II), which also carries out the serial communication. This computer enabled us to develop the control program easily because we could load the BASIC programs directly from PC without removing the microcomputers from the circuit board. So we could develop the program and repeatedly carrying out the gliding experiments.

Control using sensor feedback needs more calculation ability. For terrain adaptive propulsion, the system is controlled by a PC with a tether. So an electrical implementation was considered about these two control systems.

The power source is composed of Ni-Cd (1.2V-7Ah) cells, which are installed in each segment. These 16 cells are connected in series. Using these batteries, 30[min] operation is possible on linoleum floor. Power supply from an outside source is also possible.

3.4 Control algorithm

The gliding configuration of the serpenoid curve is the most fundamental vibratory motion of the actuator because each joint angle vibrates in a sine wave. And it decreases the calculation load remarkably.

The conceptual scheme of control algorithm is illustrated in Fig.5(a). The bending angle of the first joint is

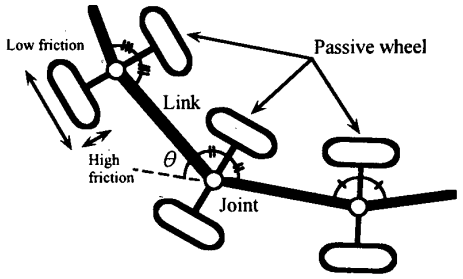

Fig.2 Kinematic model

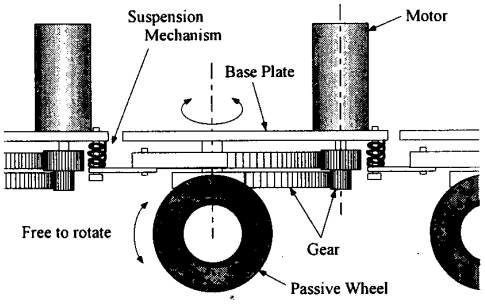

Fig.3 Mechanism of one unit

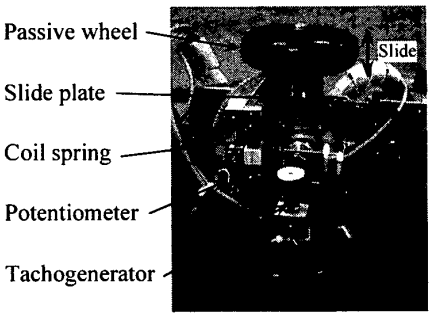

Photo.2 Bottom view of the sensor installed joint

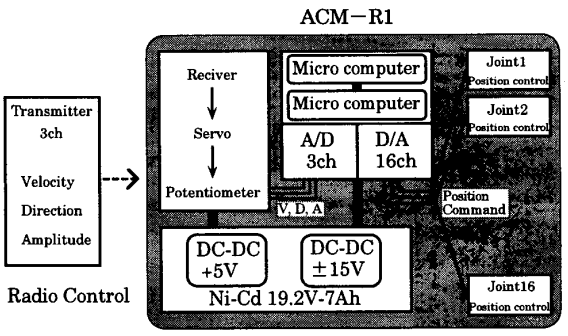

Fig.4 Configuration of the control system

stored in data array and the serpentine motion is generated by shifting it backward at fixed time intervals. It is possible to control the gliding velocity V_s without changing the gliding configuration by adjusting the time which passes in program against the actual time. By applying a bias to change the center of the sine wave vibration, the control of the gliding direction is realized. When the additional bias is 0, the standard of the curvature is straight. If the bias is constant, the standard of the curvature becomes a circular arc. While the maneuvering of the creeping machine is apparently complicated, this steering method resembles that of a car.

It is also possible that parameter A, the amplitude of the bending angle, changes the gliding configuration. By increasing the amplitude, the winding angle become larger for the creeping configuration (eqn(2)).

Photo.3 shows overview of ACM-R1 and Table.1 indicates its specifications.

4. Propulsion experiments

In order to confirm the realization of the creeping motion, propulsion experiments were carried out on linoleum flooring. The gliding configuration is fixed with l=L/4 so that one serpenoid period corresponds to the length of the body L. It was determined by considering the link length and the discrete error, and was used for all experiments.

For example, parameters are set as A=22[deg] (α=56[deg]) and T=4.2[s], the gliding velocity obtained by experiment was 0.5 [m/s]. It was only 5% lower than theoretical velocity. Therefore, the creeping motion performed by mechanical model agrees with the theory well.

By decreasing the period, propulsion of 1.0 [m/s] was achieved. It was 2 times faster than the maximum velocity of ACM III. Notice that the maximum speed is not regulated by the power of the actuator, but is rather regulated by the limits of software and batteries. Therefore, the maximum gliding speed can be increased by improving these in the future. It was also possible to change the velocity from low to high smoothly without changing gliding configuration. And it was confirmed that regression was realized by opposite data shifting. This is the clear disproof of popular belief that "Snakes cannot go backwards because they hook their scales into the ground for friction".

For gliding direction control, the steering operation was confirmed by changing the bias value. If there is a space double the distance of the trunk length, then it is possible to turn 90[deg] from the gliding direction. So maneuvering of the creeping motion was very controllable.

The gliding experiment on asphalt and carpet, which have a little roughness and comparatively large rolling resistance was performed as well. It was verified that propulsion was still possible by adjusting the amplitude of the curvature.

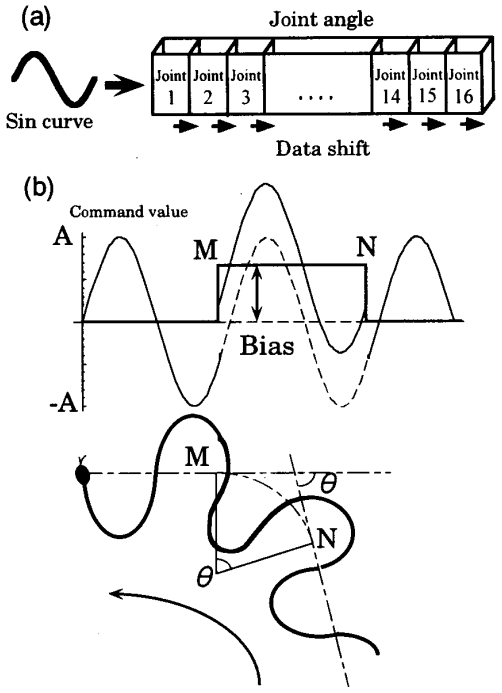

Fig.5 (a) Control algorithm (b)Steering motion

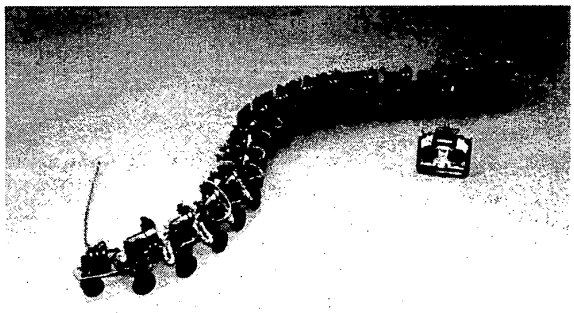

Photo.3 ACM-R1

Table.1 Specifications of ACM-R1

No. of Unit	16
Dimension	2430×175×220(mm)
Weight	28 (kg)
Actuator	50W DC Servo Motor ×16
Battery	Ni-Cd 19.2V-7Ah

5. Gliding experiments on ice

The gliding tests were carried out on ice in order to verify that the creeping locomotion was the same principle as that of skating.

The frictional property is added by replacing the passive wheels with skate edges. The experiment was performed by using 2 kinds of edges A, B for examining the difference between the motions as a function of the friction coefficient ratio. Fig.6 shows the shapes of the edges. Both of A, B have sharp edges. The frictional force was measured in a preliminary experiment and its results as well as that of the passive wheel are indicated in Table.2. In order to concentrate the weight on the contact point with ice, edge B has a circular blade. Ice is easily melted by high pressure, therefore normal friction coefficient is larger than that of edge A.

The gliding experiments were carried out by setting the winding angle α=55[deg] as one example. With edge A, there was slippage in the normal direction. Only bending motion of the trunk was observed and propulsion was limited.

With edge B, it was possible to propel smoothly same as on the ground without sideslip. The gliding speed was approximately 0.5 [m/s]. (Photo.4) It was verified that the maneuvering of creeping motion was completely controllable like on the ground using passive wheels.

However, high-speed locomotion like that of skating by a human was impossible, because the total length of the contact point with the ice is much larger than that of a normal skating human. And the weight of ACM-R1 is much smaller than a human. So it is difficult to melt ice. Therefore, it was not possible to make μ_t small like in the case of normal skating or passive wheels, so the gliding velocity is low. More examination of the edge's shape or heating of the edge is necessary for the high-speed locomotion.

From the experiments above, the characteristics of creeping locomotion was demonstrated. It depends on the friction coefficient ratio.

6. Terrain adaptive locomotion

It is generally known that snakes change the winding angle in order to adapt themselves to the friction coefficient ratio. For example, the snake increases the winding angle on the sloping surface or on surface where slippage occurs easily in the normal direction in order to increase tangential force.

In this chapter, we introduce this phenomenon into a control method as terrain adaptive function. However, it is difficult to change the friction coefficient ratio without restrictions. So we performed slope climbing experiments as one example of terrain adaptation. It can be regarded as the case in which the friction coefficient ratio changes. And the

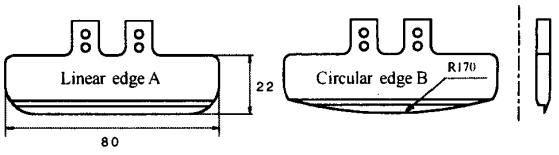

Fig.6 Geometry of the edge A,B

Table.2 Kinetic friction coefficient

	μ_t	μ_n	μ_t/μ_n
Edge A	0.06	0.14	0.43
Edge B	0.05	0.43	0.12
Wheel	0.01	0.46	0.02

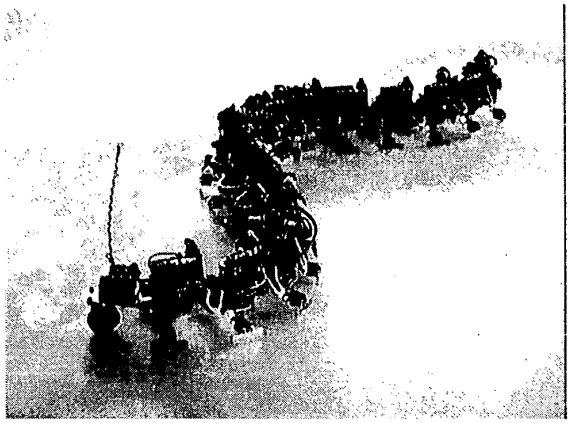

Photo.4 Experiment on ice

criterion for evaluation of the adaptation is the maximization of the propulsive velocity V_x, that is one of the most fundamental considerations for mobile robots.

To begin with, the gliding experiment on the horizontal surface is carried out, and the relationship between propulsive velocity and winding angle is clarified experimentally. And the optimized winding angle is derived. It is compared with the theoretical result.

Next, a control method which adaptively chooses optimum winding angle on sloping surface is proposed and the effectiveness of it is confirmed by experiment.

6.1 Relationship between V_x and α

First, let us discuss the relationship between propulsive velocity and winding angle qualitatively assuming that the gliding velocity v_s is constant.

If the winding angle increases, the tangential force which drives the trunk along the body axis also increases (eqn.(5)). As a result, creeping motion is generated smoothly. However, the propulsive velocity V_x is de-

creased because of the decrease in travelling ratio geometry (eqn.(4)). Thus the optimum winding angle which maximizes V_x is the minimum value obtained by the condition without slippage (eqn(6)).

The experiments were performed as follows; a theoretical gliding velocity V_s determined by eqn(3) was set, and next the gliding velocity obtained by the experiment V_{SE} was measured. The normal force and motor current were measured at same time. Next, V_s was changed and the same procedures for the experiments were carried out. V_s and α were varied from 0.1 to 1.0[m/s], from 13 to 89[deg] respectively.

Measurement of the V_s change enabled the examination of the dynamic effect such as inertial force caused by the increase of V_s. Next, normalization is performed for V_{SE} in order to examine the experimental result.

$$V_{XN} = \frac{V_{SE}}{V_S} \cdot \frac{X(l)}{l} \tag{7}$$

The relationships between V_{XN} and α is shown in Fig.7, and typical results of F_n are indicated in Fig.8(a),(b).

Concerning the dynamic effect, it can be neglected because the relationship has similar tendency regardless of V_s change. Therefore there were no problems if it was examined only by static kinematics.

From Fig.7, it can be seen that the mean value of V_{XN} becomes maximum at α=43[deg].

In the large α area, V_{XN} agrees with theoretical value well. At the same time, measured distribution of F_n also agrees with the theoretical shape of the graph well (Fig.8(b)). It takes the maximum value at point O as illustrated in Fig.1, though there is a little phase delay in the experimental result. On the contrary, V_{XN} rapidly decreases in the small α area, and does not agree with the theoretical results. In this area, F_n takes the form of a trapezoidal shape shown in Fig.8(a) for example. This is because the hardware current limitation for the actuator. In spite of satisfying the condition obtained by eqn(6) and enough actuator power to generate propulsive force, there was no propulsion of the trunk. There are two possible reasons for this disagreement.

One is mechanical problems. When the winding angle is small, the serpentine motion is absorbed because of the existence of gear backlash and play in the suspension mechanism at each joint. As a result, the body cannot generate the effective propulsive force.

The second reason is the difference of the analysis assumption. In theory, the torque distribution of the trunk is determined independently from the gliding configuration. Equation (6) is derived by using this assumption. However, when the mechanical model is actually controlled, it is impossible to control gliding morph independently from the torque distribution. The torque distribution correlates closely with the gliding morph. It is also impossible for

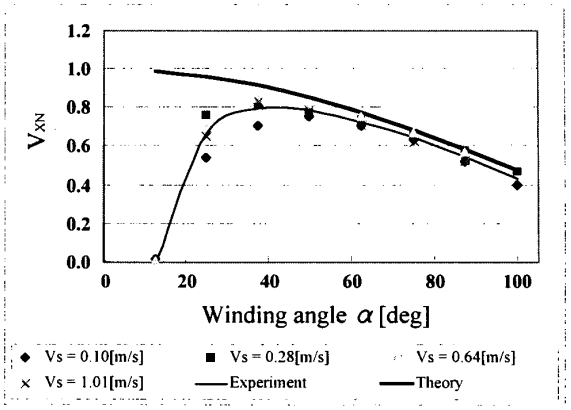

Fig.7 Winding angle vs. normalized propulsive velocity on flat surface.

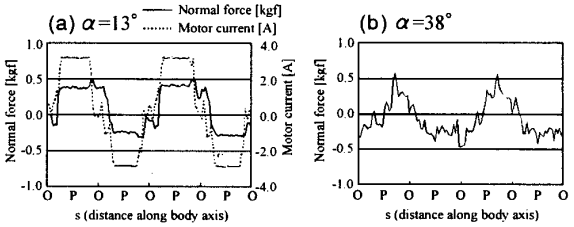

Fig.8 Distribution map of normal force

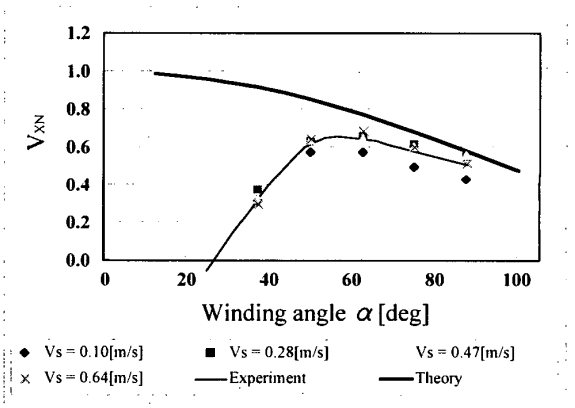

Fig.9 Winding angle vs. normalized propulsive velocity on sloping surface.

ACM-R1 to control actuator's torque because the only controllable quantity is position. Therefore, the torque distribution was changed by the decrease of the winding angle, and the needed actuator torque exceeded the current limit.

It is confirmed that the propulsive velocity decreases at small winding angle due to the hardware constraints of the experimental model. And the conventional theory could

not be applied in this case. In order to reflect actual conditions more, another analysis is needed, which considers the relationships between torque and gliding morph.

However considering the results shown in Fig.7, from the control aspect, we have obtained very useful results. That is the existence of the optimum winding angle. The same experiments were carried out on a 4[deg] sloping surface, and the results are shown in Fig.9. The optimum α on the slope was 56[deg], which is greater than on horizontal surface. This result agrees with the real snake's phenomenon.

6.2 Slope climbing experiment

In this chapter, a control method that adapts the winding angle is proposed.

The proposed control method is where the winding angle is changed in small amplitudes during the creeping motion. If the propulsive velocity is increased, chooses it as the new winding angle. It is the method that adapts the winding angle asymptotically in order to always raise the propulsive velocity shown in Fig.9. This control method enables adaptive glide on the different friction coefficient ratio surface. Therefore, by the introduction of this control method, it is able to creep on ice with edge A.

Climbing experiments from horizontal surface to a slope were carried out using this control method. Initial winding angle was set at 20[deg]. At first, it was impossible to climb the slope because of the slippage in the normal direction and even regression was observed. In a short time, however, the winding angle gradually increased and climbing was achieved (Photo.5).

By this experiment, realization and effectiveness of adaptive control method by changing the winding angle were verified.

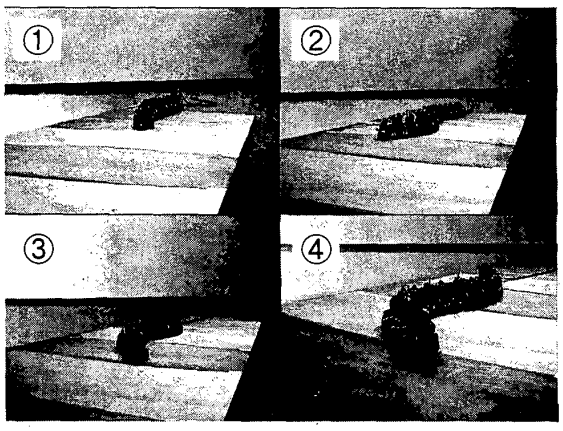

Photo.5 Terrain adaptive propulsion

7. Conclusions

In this paper, self-contained active cord mechanism ACM-R1 was newly developed for the purpose of engineering application of the creeping motion and verification by the mechanical model. In comparison with the past model ACM III, the new model realized self-containment as well as remarkably higher performance. We believe that it is extremely important for practical robotics to construct actual experimental systems using available devices in contemporary technology.

It was verified that the principle of the creeping locomotion is equivalent to that of skating by experiments on ice using ACM-R1. Next, the relationship between propulsion velocity and winding angle was clarified experimentally, and compared with theory. The results show that there was a case that is not applicable, in which the gliding configuration and torque distribution were determined independently. And a control method, which adaptively chooses the optimum winding angle depending on the friction coefficient ratio, was proposed. The effectiveness was confirmed by climbing experiments on a slope.

We have plans for various future work. For example, investigations of the creeping motion which minimizes the energy consumption, and adaptive control using information from the normal force sensor. Concerning theory, it is necessary to examine a new gliding theory with the torque distribution, which depends on the gliding configuration.

Acknowledgments

The authors would like to thank Kanagawa skate rink which offered the field of the experiment.

This research is supported by JSPS Research Fellowships for Young Scientists and The Grant-in Aid for COE Research Project of Super Mechano-Systems by the Ministry of Education, Science, Sport and Culture.

References

[1] Shigeo Hirose : "Biologically Inspired Robots (Snake-like Locomotor and Manipulator)", Oxford University Press,1993

[2] A. Naito and S. Ma : "Analysis of Creeping Locomotion of Snake-like Robots", in Proc. 3nd Asian Conf. on Robotics and Its Application, pp.393-398 ,1997

[3] Shugen MA : "Analysis of Snake Movement Forms for Realization of Snake-like Robots", in Proc. IEEE International Conference on Robotics and Automation, pp.3007-3013, 1999

[4] E.F.Fukushima, T.Tsumaki, S.Hirose : "Development of a PWM DC Motor Servo Driver Circuit", in Proc. of RSJ95, pp.1153-1154, 1995(in Japanese)